FISEVIER

Contents lists available at ScienceDirect

Chemical Engineering Journal

journal homepage: www.elsevier.com/locate/cej



TiO₂@C nanosheets with highly exposed (0 0 1) facets as a high-capacity anode for Na-ion batteries



Qi Zhang^a, Hanna He^a, Xiaobing Huang^b, Jun Yan^a, Yougen Tang^{a,c}, Haiyan Wang^{a,c,*}

- a Hunan Provincial Key Laboratory of Chemical Power Sources, Hunan Provincial Key Laboratory of Efficient and Clean Utilization of Manganese Resources, College of Chemistry and Chemical Engineering, Central South University, Changsha 410083, PR China
- ^b College of Chemistry and Chemical Engineering, Hunan University of Arts and Science, Changde 415000, PR China
- ^c Hunan Zhongda Haoneng Co. Ltd., Changsha 410000, PR China

ARTICLE INFO

Keywords: Sodium-ion battery Titanium dioxide Exposed (0 0 1) facets Carbon coating Rate performance

ABSTRACT

Surface engineering plays a key role in enhancing the electrochemical performance for energy storage materials. Herein, TiO_2 nanosheets with highly exposed (0 0 1) facets are synthesized by a HF-induced hydrothermal process and $TiO_2@C$ composite is obtained by the following carbonation reaction of phenolic resin. As indicated, TiO_2 nanosheets are averagely 50 nm wide and 4 nm thick and a homogeneous and ultrathin carbon layer (3 nm) is coated on the nanosheets. When used as an anode in Na-ion batteries, it delivers a high stable specific capacity of 264.9 mAh g⁻¹ after 100 cycles at 100 mA g⁻¹ and maintains a considerable specific capacity of 92.9 mAh g⁻¹ after 4000 cycles even at a high current density of 5 A g⁻¹. The superior sodium storage performance and ultralong cycling life of the as-prepared $TiO_2@C$ should be mainly attributed to the synergistic effect of high-energy facet designing and gorgeous carbon layer coating.

1. Introduction

Sodium-ion batteries (SIBs) have been regarded as the most promising candidate as a substitute to lithium-ion batteries (LIBs) for nextgeneration batteries because of the inexhaustible sodium resources and the similar intercalation electrochemistry to LIBs [1,2]. However, the ionic radius of sodium ion (0.102 nm) is much larger than that of lithium ion (0.076 nm) leading to the lower energy density and poorer cyclic life [3]. Recently, layered transition-metal oxides (e.g., Na_xCoO₂ [4], and Na_xFe_{1/2}Mn_{1/2}O₂ [5]), polyanionic phosphates (e.g., NaFePO₄ [6], and $Na_3V_2(PO_4)_3$ [7]), vanadates (e.g., V_2O_5 [8], NaV_3O_8 [9], NaV₆O₁₅ [10]) and Prussian blue analogues (e.g., Na₄Fe(CN)₆ [11], and Na₂FeMn(CN)₆ [12]) have been studied as cathode materials. However, the choice of high-performance anode materials is greatly limited since the common anode materials in lithium ion batteries, graphite and silicon, show very poor sodium storage ability [13]. Nowadays, the studied anode materials for SIBs can be classified into alloy compounds [14–16], conversion materials [17,18], and insertion-type materials [8,19,20] according to the charge-discharge mechanisms. Although exhibiting high sodium storage capabilities, the alloy compounds and conversion materials tend to be pulverized and inactivated because of the large volume expansion during the cycling, thus resulting in rapid capacity fading [21-23].

Among the insertion-type materials, TiO₂ has drawn enormous attention for its natural abundance, appropriate voltage plateau and structural stability during the sodiation/desodiation process [24]. TiO₂ has a variety of crystal phases mainly including rutile, anatase, brookite and hollandite. Anatase shows better sodium storage ability than the other phases by the suitable stacking of TiO₆ octahedra, forming Na⁺ pathways with a less diffusion resistance [25]. However, the inherent semiconductor characteristic and sluggish Na+ diffusion of pristine TiO₂ result in inferior rate performance. To solve the above issues, relevant strategies including nanostructure construction [26], element doping [27,28], and conductive carbon coating [13] have been widely reported. Some pioneering works reveal that high-energy facet orientation of nanoparticles is a critical factor for rapid ions insertion/ extraction [29]. For anatase TiO2, the average surface energies of (0.01), (1.00) and (1.01) facets are $0.90\,\mathrm{J\,m^{-2}}$, $0.53\,\mathrm{J\,m^{-2}}$ and $0.44 \,\mathrm{J\,m^{-2}}$, respectively, and the bandgap of $\mathrm{TiO_2}$ with (0 0 1) facet is much lower than those of (101), (010) and (111), indicating the higher activity of (0 0 1) facet [30]. Longoni et al. reported that TiO2 with exposed (0 0 1) and (1 0 0) high-energy facets showed the higher specific capacity (180 mAh $\rm g^{-1}$ at 0.1 C) compared to $\rm TiO_2$ with exposed (1 0 1) and (0 1 1) facets (88 mAh $\rm g^{-1}$ at 0.1 C) [31]. Further calculation results show that the energy barrier for Na⁺ insertion into the (0 0 1) surface is lower than that into the (1 0 1) surface, indicating

^{*} Corresponding author at: Hunan Provincial Key Laboratory of Chemical Power Sources, Hunan Provincial Key Laboratory of Efficient and Clean Utilization of Manganese Resources, College of Chemistry and Chemical Engineering, Central South University, Changsha 410083, PR China.

E-mail address: wanghy419@126.com (H. Wang).

that the $(0\ 0\ 1)$ direction is more accessible for Na⁺ diffusion [32]. However, high-energy facets tend to vanish rapidly during the synthesis. Some kinds of capping agents such as HF and NH₄F have been proposed to stabilize the high-energy facet [33]. For example, Lou et al. prepared TiO₂ hollow nanospheres highly exposed with $(0\ 0\ 1)$ active facets using HF as capping agent through a template method for lithium storage, which delivered a reversible capacity of 148 mAh g⁻¹ after 200 cycles at 1 C [34]. It should be noted that highly exposed high-energy facet is fragile and also easy to lose its activity after continuous cycles [35,36]. Surface engineering with a thin carbon or other oxides coating can stabilize such high-energy facets [37]. For this reason, it is believed that sodium storage performance of TiO₂ could be significantly improved if combining the high-energy facet tuning and advanced carbon coating.

In this work, we first synthesized well-dispersed anatase ${\rm TiO_2}$ nanosheets with highly exposed (0 0 1) facets using hydrofluoric acid as the shape-controlling agent and then the uniform thin carbon layer was successfully coated on the (0 0 1) surface of ${\rm TiO_2}$ using phenolic resin as the carbon source. The carbon layers formed by pyrolysis of phenolic resin play a role not only in improving the electrical conductivity but also in preserving the (0 0 1) facets during the synthetic process and charge-discharge cycles. Benefiting from the specific two-dimensional nanostructure, the as-prepared carbon coated ${\rm TiO_2}$ nanosheets showed superior sodium storage performance.

2. Experimental section

2.1. Synthesis of carbon coated TiO2 nanosheets

 TiO_2 nanosheets (TS) were synthesized using a hydrothermal method [38]. In a typical process, 20 mL of tetrabutyl titanate was added into an 80 mL Teflon-lined autoclave, and subsequently 2.4 mL of hydrofluoric acid solution (40 wt%) was slowly injected into the above solution. After continuous stirring for 30 min at room temperature, the autoclave was sealed and maintained at 180 °C for 24 h. The white products were collected by vacuum filtration and washed with ethanol for several times, then dried in air at 65 °C overnight. TiO_2 bulks (TB) were obtained by the similar process with 2.4 mL of distilled water substituted for HF solution.

Carbon coated $\rm TiO_2$ nanosheets (CTS) were prepared according to the following procedure. Firstly, 0.8 g of as-prepared $\rm TiO_2$ nanosheets is dispersed in 56 mL of distilled water by ultrasonication for 30 min, then 2 mL of 0.01 M cetyltrimethylammonium bromide (CTAB) solution and 0.2 mL of concentrated ammonia solution (28 wt%) were dropped into the suspension. After stirred for another 30 min, 0.1 g of resorcinol and 0.14 mL of formaldehyde solution (37 wt%) were added. The suspension was stirred for 24 h without interruption. A dark brown precipitate was obtained by centrifugation and washed with distilled water for several times. After dried at 65 °C, the obtained powder was calcined in Ar at different temperature (600 °C, 700 °C and 800 °C, denoted as CTS–600, CTS–700 and CTS–800, respectively) for 2 h with a heating rate of 5 °C min $^{-1}$.

It was proved that $~700\,^{\circ}\text{C}$ is the optimized temperature. Accordingly, for comparison, TS–700 and TB–700 were also synthesized by heating TiO $_2$ nanosheets and TiO $_2$ bulks at 700 $^{\circ}\text{C}$ for 2 h in Ar, respectively.

2.2. Characterization

The powder X-ray diffraction (XRD) patterns were collected using a Bruker D8 X-ray diffractometer with monochromatized Cu K α radiation (the wavelength of 1.5406 Å). The morphologies of the products were characterized by scanning electron microscopy (SEM, Nova NanoSEM 230) and transmission electron microscopy (TEM, JEOL JEM-2100F). The microstructure was further measured by high resolution transmission electron microscopy (HRTEM). Raman spectra were tested by a

LabRAM Aramis (HORIBA Jobin Yvon) spectrometer using an excitation wavelength of 633 nm. The carbon contents were determined with thermogravimetric analysis (TGA) using a STA 449 C thermoanalyzer at a heating rate of 5 °C min $^{-1}$ from 25 to 800 °C in air. DC electrical conductivities were tested by a four-point probes instrument (ST-2722, Jingge). X-ray photoelectron spectroscopy (XPS) was performed by utilizing a K-Alpha1063 spectrometer with Al K α radiation at 6 mA and 12 kV.

2.3. Electrochemical measurements

To fabricate the test electrodes of Na-ion batteries, the as-prepared anode materials, conductive additive (acetylene black) and binder (polyvinylidene fluoride, PVDF) were mixed in a weight ratio of 7:2:1 with N-methyl-2-pyrrolidone (NMP) as the dispersing agent. The slurry was uniformly pasted onto a copper foil, then dried at 80 °C under vacuum until the solvent evaporated completely. The average mass loading on the copper foil was about 1.5 mg cm⁻². CR2016 coin-type cells were assembled by using the home-made sodium metal disk as the counter electrode and the glass fiber as the separator. A solution containing 1 M NaPF₆ dissolved in a mixture of ethylene carbonate (EC), diethyl carbonate (DEC) and dimethyl carbonate (DMC) with a volume ratio of 1:1:1 was used as electrolyte. Galvanostatic charge/discharge tests were performed on a Neware CT-3008W battery testing system at a potential range of 0.01-3.00 V under various current densities. Cyclic voltammetry (CV) measurements were conducted on a CHI660D electrochemical workstation between 0.01 and 3.00 V. Electrochemical impedance spectroscopy (EIS) was measured by a Princeton Parstat2273 workstation with a frequency range from 105 Hz to 0.01 Hz. Before the EIS tests, the cells were activated by five discharge-charge cycles at 50 mA g⁻¹ and then charged to 0.8 V.

3. Results and discussion

XRD patterns of the as-synthesized samples are shown in Fig. 1. As seen, the diffraction peaks can be well indexed to the standard card of anatase ${\rm TiO_2}$ (JCPDS No: 21-1272) and no other impurity peaks indicate the high purity of the as-prepared samples. Among all the samples, impurity peaks are observed only in TB–700 in Fig. S1 which was partially transferred into rutile phase after calcining at 700 °C. The diffraction peaks of other calcined samples remain at the original positions and become sharp and narrow, representing better crystallization. The peaks of CTS–700 are broader than those of TS–700

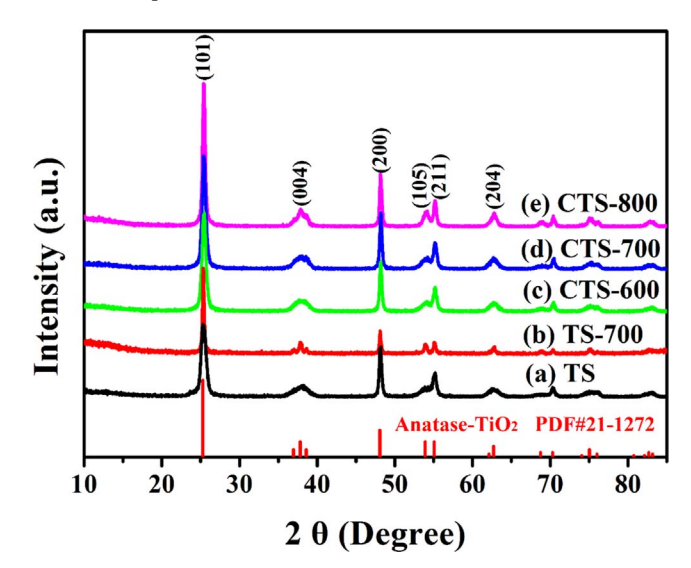


Fig. 1. XRD patterns of (a) TS, (b) TS-700, (c) CTS-600, (d) CTS-700, (e) CTS-800, (f) TB and (g) TB-700.

Download English Version:

https://daneshyari.com/en/article/6464977

Download Persian Version:

https://daneshyari.com/article/6464977

<u>Daneshyari.com</u>